03

Investigation of the influence of the direction of the incoming flow relative to the plane of the three-cylinder rotor on the aerodynamic coefficients

© A.Zh. Tleubergenova, N.K. Tanasheva, K.M. Shaimerdenova, A.N. Dyusembaeva, A.Zh. Satybaldin

Buketov Karaganda University, Karaganda, Republic of Kazakhstan
E-mail: nazgulya_tans@mail.ru

Received December 28, 2022
Revised January 17, 2023
Accepted January 17, 2023

Experiments have been carried out to study the influence of the direction of the incoming flow relative to the rotor plane on the values of the drag coefficient of a multi-blade rotor layout with power elements in the form of rotating cylinders of variable cross-section. It is shown that the drag force of the multipath depends on the Reynolds number, and practically remains constant in the range of Reynolds numbers $(16-50)\cdot 10^4$ .According to the results of a series of experimental data, the dependences of the thrust coefficient of the multipath rotor on the Reynolds number and the installation angle of the airflow were also calculated and constructed. It is established that the coefficient of thrust of the rotor decreases with an increase in the Reynolds number.

Keywords: rotor, Reynolds number, drag force coefficient, thrust force coefficient, WEUC (wind energy utilization coefficient).

DOI: 10.21883/TPL.2023.04.55867.19472

It follows from experience that the results of experimental studies of a model do not always match the data for full-scale demonstration facilities. This is attributable to the fact that the flow past a model in an aerodynamics laboratory environment differs from the flow past a body in real-world environments. In order to estimate the aerodynamic parameters of a full-scale unit based on the obtained aerodynamic characteristics of a model, one needs to known the laws of transition from a model to full-scale demonstration facilities [1–3].

The aim of the present study is to examine the influence of the airflow incidence angle on the aerodynamic characteristics of a three-cylinder rotor. A three-cylinder rotor operates based on the Magnus effect, which is the result of a combined action of such physical phenomena as the Bernoulli effect and the formation of a boundary layer in a medium around an object.

Experimental studies into the influence of the incidence angle of flow on the aerodynamic characteristics of a single cylinder were performed in [4].

The next series of experiments were also conducted in the working section of a wind tunnel with a three-cylinder rotor model and were aimed at examining the influence of the flow direction on the aerodynamic characteristics of the device under study [4–6]. Experimental studies were carried out at the Aerodynamic Measurements Laboratory. The model was mounted in the working section of a T-1-M wind tunnel (this working section has diameter $D = 0.5\,\text{m}$ and length $L = 0.8\,\text{m}$) that was secured by thin metal braces to the frame of a three-component aerodynamic balance. A three-component balance allows one to measure the drag and lift forces with a fairly high accuracy. A spring balance connected to a pulley on the rotation axis of the wind wheel was used to measure the thrust force. Its spring deformed in proportion to the applied force produced by the rotating rotor. The degree of spring deformation corresponds to the force magnitude. Measurements were performed several (at least five) times; the measurement error was 3%. The diameter of the rotor model was 45 cm, the diameter of the cylinder with a variable cross section was 5 cm, and its length was 20 cm. Figure 1 shows the diagram and the photographic image of the experimental three-cylinder rotor.

The airflow incidence angle assumed the values of $\alpha = 0$, 15, 30, 45, 60°. Since the rotor efficiency decreased sharply at $\alpha > i60°$, these incidence angles were not probed experimentally.

Drag coefficient C_x, thrust force coefficient C_m, and Reynolds number Re were calculated using the following formulae [7,8]:

$$C_x = \frac{\Delta F_x}{\rho \frac{u^2}{2} S}, \quad C_m = \frac{F_m}{\rho \frac{u^2}{2} S}, \quad \text{Re} = \frac{ud}{\nu}, \tag{1}$$

where ΔF_x is the drag force [N], F_m is the thrust force [N], ρ is the air density [kg/m^3], u is the flow velocity [m/s], S is the rotor midsection area [m^2], d is the diameter [m], and ν is the kinematic viscosity of air [Pa · s]. The flow velocity varied from 5 to 15 m/s.

The blockage coefficient was calculated as

$$B_R = \frac{S}{S_t}, \tag{2}$$

where S_t is the area of the working section of the wind tunnel [m^2].

The influence of the flow incidence angle on the rotation rate of the main rotor shaft at three different air velocities was examined in the same series of experiments (Fig. 2).

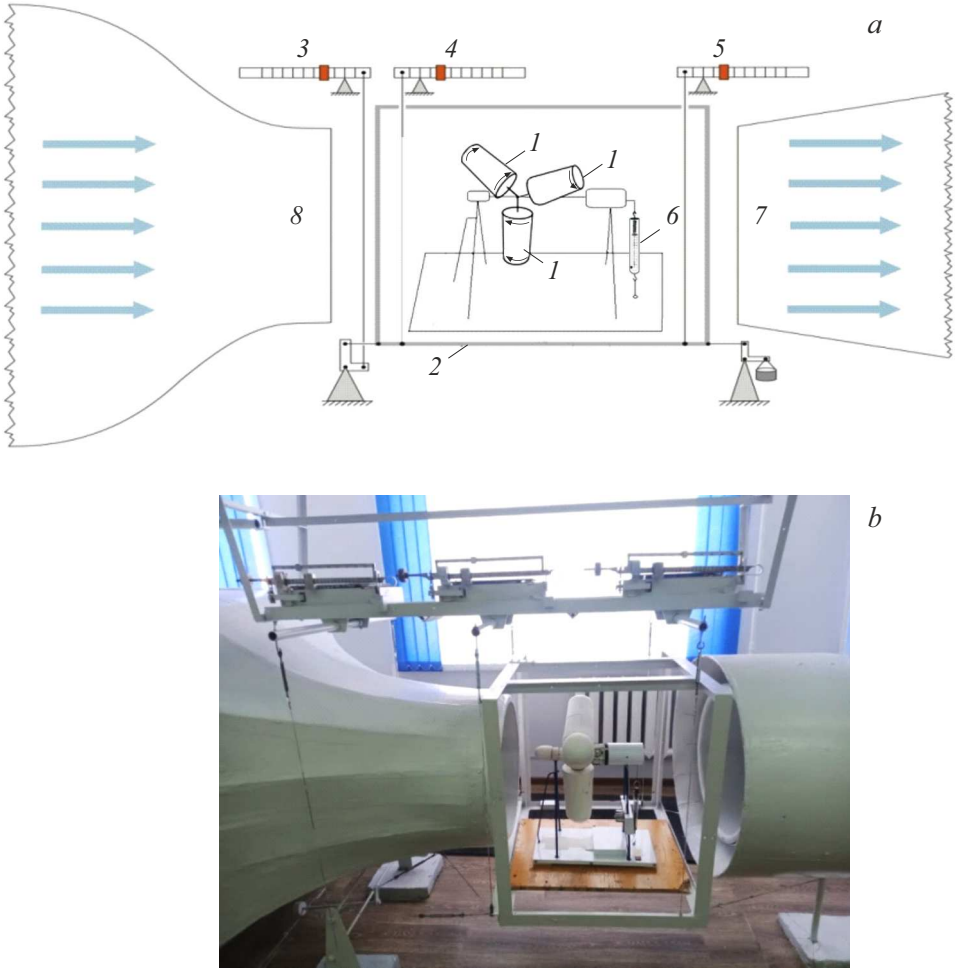

Figure 1. *a* — Positioning of the experimental three-cylinder rotor in the working section of the T-1-M wind tunnel. *1* — Wind turbine cylinders, *2* — frame onto which the model with an aerodynamic balance is secured, *3* — balance measuring the drag force, *4*, *5* — balance measuring the lift force, *6* — spring balance (measuring the thrust force), and *7*, *8* — wind-tunnel contraction and diffuser. *b* — Photographic image of the experimental three-cylinder rotor in the working section of the T-1-M wind tunnel.

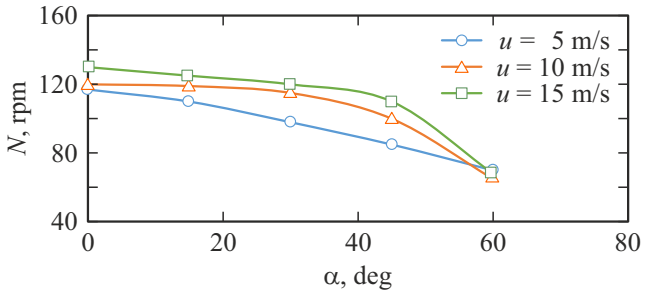

Figure 2. Dependences of the rotation rate of the main shaft of the rotor model on flow incidence angle α at different velocities.

The obtained plot (Fig. 2) demonstrates that the rotation rate of the main rotor shaft decreases gradually as the flow incidence angle increases to $\alpha = 45°$; at greater angles, a more rapid reduction is observed. This type of variation of the rotation rate with wind direction may be attributed to the effect of flow rearrangement (variation of the model rotor midsection area with position angle relative to the general wind direction).

Graphical dependences of the drag force coefficient and the thrust force coefficient of the three-bladed rotor model on the dimensionless velocity (Reynolds number) with the general wind direction varying within a fairly wide range of incidence angles (from 0 to 60°) were plotted by processing the obtained extensive experimental data set with the use of similarity theory elements. These dependences are presented in Figs. 3, *a*, *b*.

It follows from Fig. 3, *a* that the drag coefficient of the three-bladed rotor model depends only weakly on the Reynolds number and remains almost constant within the studied range of Reynolds numbers ($(16-50)\cdot 10^4$). The dependence of this coefficient on the flow incidence angle is nonmonotonic: it decreases as α increases to 45°, but grows at greater α angles. A physical interpretation of this behavior was proposed in discussion of measurements of

Wind energy utilization coefficient of the three-cylinder rotor at different air flow velocities

u, m/s	ρ, kg/m^3	R, m	S, m^2	N_{wf}, W	m	M_c, N · m	n	ω_c, rad/s	M_r, N · m	N, rpm	ω_r, rad/s	N_r, W	ξ
5	1.225	0.22	0.15	11.6	3	0.5	120	12.56	4	50	5.2	20.9	0.18
9	1.225	0.22	0.15	67.8	3	1.2	170	∼ 17.79	10	75	7.8	78.5	0.21
13	1.225	0.22	0.15	204.5	3	2	300	31.4	15	156	16.3	244.92	0.27
15	1.225	0.22	0.15	314.1	3	3	350	∼ 36.63	17	238	24.9	423.48	0.29

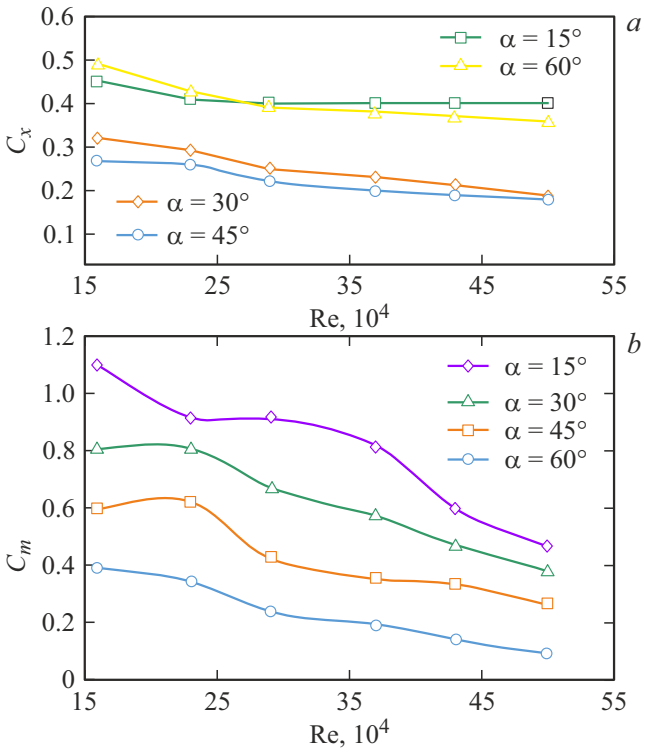

Figure 3. Dependences of the drag coefficient (a) and the thrust force coefficient (b) of the three-bladed rotor model on the Reynolds number at different flow incidence angles.

the dependence of the drag force on the flow incidence angle. The drag force remains almost unchanged at low incidence angles (0−15°) and starts decreasing gradually at greater angles (15−40°). At anglers α in excess of 45°, the drag force grows gradually. In physical terms, this complex shape of the dependence may be attributed to the rearrangement of the velocity field of air flow past the wind turbine occurring when the model is rotated by angle α varying from 0 to > 45°.

As the Reynolds number grows, the drag coefficient decreases slightly at all the considered incidence angle values (Fig. 3, a). This is due to the fact that inertia forces dominate at higher Reynolds numbers over viscous forces emerging in the motion of a fluid owing to the momentum transfer in a direction perpendicular to the motion direction.

Areas of low pressure form in a turbulent air flow as a result of interaction with secondary flows produced by rotating cylinders. The volume of these areas varies with flow incidence angle [4–6,9,10].

Therefore, the thrust force of the wind turbine model, which is caused by the incident flow, is produced due to the pressure difference on the surface of rotating cylinders.

It follows from Fig. 3, b that the thrust force coefficient depends functionally on the model position angle and on the Reynolds number. The thrust force coefficient decreases with increasing Reynolds number. This is attributable to the fact that the bearing member of the wind engine operates normally at flow incidence angles varying from 0 to 45°, but the operation efficiency drops sharply at angles greater than 45°.

Wind energy utilization coefficient (WEUC) ξ is calculated below. This coefficient depends on the surface motion velocity and the wind direction.

The following formula was used to determine it:

$$\xi = \frac{N_r - N_c}{N_{wf}}, \tag{3}$$

where $N_c = mM_c\omega_c$ is the cylinder rotation power, m is the number of cylinders, M_c is the moment of forces acting on a rotating cylinder, ω_c is the angular rate of rotation of a cylinder, $N_{wf} = \frac{\rho u^3 S}{2}$ is the wind current power, ρ is the air density in the incident flow, $S = \pi R^2$ is the rotor midsection area, R is the rotor radius, u is the incident flow velocity, $N_r = M_r\omega_r$ is the rotor rotation power, M_r is the moment of forces acting on a moving rotor, n is the number of cylinder revolutions, N is the wind wheel rotation rate, and ω_r is the angular rate of free rotation of a rotor (or $N_r = M_r \frac{2\pi n_1}{60}$).

At an air flow velocity of 5 m/s, we obtain WEUC $\xi = 0.18$ for the three-cylinder rotor.

The experimental data needed to determine the wind energy utilization coefficient are listed in the table.

Thus, the results of our experiments revealed that the studied rotor design differs from the other known designs in providing a more active capture of the air flow by rotating cylindrical elements (i.e., the emerging additional lift force is utilized). The potential for adjustment of the cross section ensures that rotating elements feature an optimum aerodynamic drag and a fairly high thrust force within a sufficiently wide velocity range. However, the thrust force decreases sharply at flow incidence angles in excess of 45°. A special device limiting the incidence angle to 45° needs to be constructed in further studies.

Funding

This study was supported financially by the Committee of Science of the Ministry of Science and Higher Education of the Republic of Kazakhstan (IRN AR14870066, „Development and Construction of an Energy-Efficient Hybrid Vertical Axis Wind Turbine with the Use of a Direct-Drive Low-Speed Electric Generator“).

Conflict of interest

The authors declare that they have no conflict of interest.

References

[1] P.N. Solyanik, M.L. Surgailo, V.V. Chmovzh, *Eksperimental'naya aerodinamika* (KhAI, Khar'kov, 2007) (in Russian).
[2] A.K. Martynov, *Prikladnaya aerodinamika* (Mashinostroenie, M., 1972) (in Russian).
[3] B.P. Khozyainov, M.A. Berezin, Vestn. Kuzbasskogo Gos. Tekh. Univ., No. 4, 38 (2000) (in Russian).
[4] N.K. Tanasheva, N.N. Shuyushbayeva, E.K. Mussenova, Tech. Phys. Lett., **44** (9), 787 (2018). DOI: 10.1134/S1063785018090134.
[5] N.K. Tanasheva, B.R. Nusupbekov, A.N. Dyusembaeva, N.N. Shuyushbayeva, Tech. Phys., **64** (7), 947 (2019). DOI: 10.1134/S1063784219070247.
[6] N.K. Tanasheva, T.O. Kunakbaev, A.N. Dyusembaeva, N.N. Shuyushbayeva, S.K. Damekova, Tech. Phys., **62** (11) 1631 (2017). DOI: 10.1134/S1063784217110299.
[7] N.M. Bychkov, A.V. Dovgal, V.V. Kozlov, J. Phys.: Conf. Ser., **75**, 012004 (2007). DOI: 10.1088/1742-6596/75/1/012004
[8] N.M. Bychkov, Thermophys. Aeromech., **12** (1), 151 (2005). https://www.sibran.ru/upload/iblock/744/744d9166b640183e4664f1552439f889.pdf
[9] C. Demartino, F. Ricciardelli, Eng. Struct., **137**, 76 (2017). DOI: 10.1016/j.engstruct.2017.01.023
[10] W. Ma, X. Zhang, J. Macdonald, L. Jin, Y. Li, J. Wind Eng. Ind. Aerodyn., **220**, 104839 (2022). DOI: 0.1016/j.jweia.2021.104839